Supplement of:

Circulation, mixing, and biogeochemical exchange in the Gulf of Taranto

Malek Belgacem[1,2]*, Florian V. M. Kokoszka[1]*, Carolina Cantoni[1], Katrin Schroeder[1], Jacopo Chiggiato[1], Stefania Sparnocchia[1], Elena Fragiacomo[1], Francesco Acri[1], Marzia Rovere[1]

[1]Consiglio Nazionale delle Ricerche-Istituto di Scienze Marine (CNR-ISMAR), Venice/Naples/Trieste/Bologna, Italy
[2]International Ocean Carbon Coordination Project (IOCCP), Institute of Oceanology, Polish Academy of Sciences, Sopot, Poland

Correspondence to: Malek Belgacem (malekbelgacem@cnr.it)

S1 Water-mass and preformed carbon

The two deep classes differ in a way that provenance alone does not explain. EMDW-ad is warmer and saltier than EMDW-r (13.74 °C and 39.03 g kg^{-1} against 13.51 °C and 38.96 g kg^{-1}), although Adriatic dense water is traditionally the colder, fresher end-member of EMDW. Terzić et al. (2025) documented warming of 0.4–0.8 °C per decade and salinization of 0.2 per decade in the deepest Southern Adriatic between 2010 and 2024, two to four times the rates observed in the northern Ionian. A recently formed Adriatic vein is therefore expected to be warmer and saltier than resident water ventilated under earlier conditions. Assuming that source properties are broadly conserved along the pathway, the observed offsets of 0.23 °C and 0.065 g kg^{-1} each correspond to roughly four years of these trends, placing EMDW-ad as the later-ventilated of the two.

The carbonate system carries an independent and consistent signal. In the Adriatic–Ionian system dense water forms by rapid winter convection; newly formed water is close to oxygen saturation at the surface but is not in equilibrium with atmospheric CO_2, so its preformed DIC is set largely by the atmospheric CO_2 concentration at the time of formation rather than by its oxygen content. Atmospheric CO_2 has risen by roughly 33 ppm over the past fifteen years, so a water mass ventilated in the early 2010s under otherwise comparable conditions would carry approximately 17 µmol kg^{-1} less DIC, and about 0.03 pH units more, than one ventilated in 2023 (Álvarez et al., 2014; Cantoni et al., 2024;

Dentico et al., 2026). Removing the estimated respiratory contribution from the measured DIC of the two deep classes, using either the Redfield et al. (1963) or the Anderson and Sarmiento (1994) C:O_2 ratio, leaves a preformed DIC offset of 12–13 μmol kg^{-1} between them.

At the rate of roughly 1.1 μmol kg^{-1} yr^{-1} implied by the recent atmospheric CO_2 increase, and assuming approximate air–sea equilibration at formation, that offset corresponds to about 10–12 years of atmospheric forcing, whereas the thermohaline offsets imply a separation of 3–6 years. Both indicators place EMDW-r as the earlier-ventilated of the two deep classes, but they differ in magnitude by a factor of two to three. The discrepancy may reflect incomplete air–sea CO_2 equilibration during rapid dense-water formation, mixing along the pathway, source-water variability, or uncertainties in the AOU-based respiratory correction and in carbonate-system buffering. No single transient tracer provides an absolute age for Mediterranean water masses; AOU combined with regional knowledge of the circulation indicates that these classes are older than the overlying layers but does not date them. The inferred timescales should therefore be read as qualitative age equivalents rather than as dated water masses.

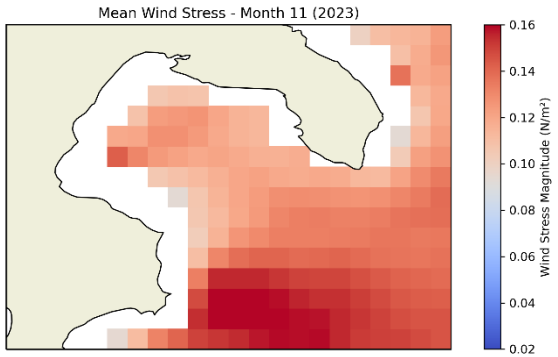
A final caution applies to the reference slopes in Fig. S2b. The upper-water DIC–AOU fit rests on n = 12 with a wide confidence interval, and the Redfield conversion must be made internally consistent before it is used quantitatively: the classical C:O_2 stoichiometry of Redfield et al. (1963) and the lower ratio proposed by Anderson and Sarmiento (1994) yield measurably different reference slopes.

Table S1: Combined (double-diffusion + internal-wave) vertical diffusive tracer fluxes across the four interfaces of interest, from deepest to shallowest. Each cell gives the flux direction (↑ upward, ↓ downward, ≈0 negligible), the flux ± 1u, the significance (robust |F|≥2u; marginal 1–2u; ns, not significant, <1u), and the dominant process (IW internal-wave, DD double-diffusion). Here u is the combined propagated and bootstrap uncertainty. Positive = upward; total (dd+iw) over a 160 m window.

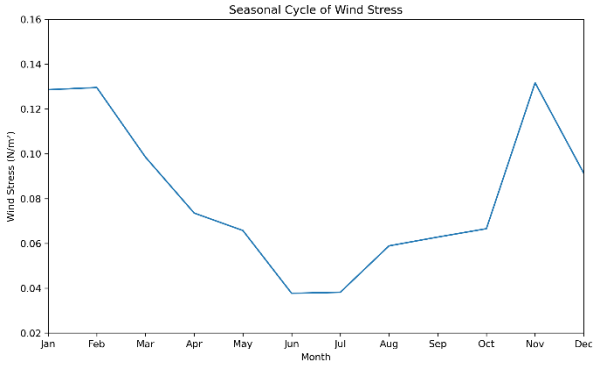
Tracer (units)	Deep interface σ_θ = 29.203 kg m^{-3} (within EMDW)	OML–EMDW-r σ_θ = 29.195 kg m^{-3}	EIW-down–OML σ_θ = 29.184 kg m^{-3}	EIW-core–EIW-down σ_θ = 29.120 kg m^{-3}
Salinity (g m^{-2} s^{-1})	↑ $+6.5\times10^{-4} \pm 1.8\times10^{-4}$ (3.5u, IW)	↑ $+2.0\times10^{-4} \pm 0.7\times10^{-4}$ (2.7u, IW)	↓ $-4.5\times10^{-5} \pm 0.3\times10^{-5}$ (15u, DD)	↓ $-1.6\times10^{-5} \pm 0.5\times10^{-5}$ (3.4u, DD)
Oxygen (μmol m^{-2} s^{-1})	↑ $+7.39\times10^{-2} \pm 2.08\times10^{-2}$ (3.6u, IW)	↑ $+2.63\times10^{-2} \pm 1.37\times10^{-2}$ (1.9u, IW)	↓ $-1.54\times10^{-2} \pm 0.10\times10^{-2}$ (15u, DD)	≈0 $-1.8\times10^{-6} \pm 1.11\times10^{-3}$ (ns)
DIC (μmol m^{-2} s^{-1})	↑ $+3.85\times10^{-2} \pm 1.18\times10^{-2}$ (3.2u, IW)	↑ $+3.71\times10^{-2} \pm 0.88\times10^{-2}$ (4.2u, IW)	↓ $-1.34\times10^{-2} \pm 0.30\times10^{-2}$ (4.5u, DD)	≈0 $+2.7\times10^{-4} \pm 5.5\times10^{-4}$ (ns)
TA (μmol m^{-2} s^{-1})	↑ $+2.15\times10^{-2} \pm 0.93\times10^{-2}$ (2.3u, IW)	↑ $+3.79\times10^{-2} \pm 0.70\times10^{-2}$ (5.4u, IW)	↓ $-0.65\times10^{-2} \pm 0.28\times10^{-2}$ (2.4u, DD)	≈0 $+6.6\times10^{-4} \pm 8.4\times10^{-4}$ (ns)

Nitrate	↓ $-3.6\times10^{-3} \pm 2.2\times10^{-3}$	≈0 $-6.5\times10^{-5} \pm$	≈0 $+6.9\times10^{-6} \pm 2.6\times10^{-4}$	≈0 $-1.3\times10^{-5} \pm 1.3\times10^{-4}$
(μmol m^{-2} s^{-1})	(1.6u, IW)	6.8×10^{-4} (ns)	(ns)	(ns)
Phosphate	↓ $-8.5\times10^{-4} \pm 4.2\times10^{-4}$	↑ $+2.9\times10^{-4} \pm$	↑ $+1.5\times10^{-4} \pm 0.4\times10^{-4}$	↑ $+4.3\times10^{-5} \pm 1.7\times10^{-5}$
(μmol m^{-2} s^{-1})	(2.0u, IW)	2.6×10^{-4} (1.1u, IW)	(3.7u, DD)	(2.6u, DD)
Silicic acid	↓ $-6.7\times10^{-3} \pm 1.6\times10^{-3}$	≈0 $+3.7\times10^{-4} \pm$	↑ $+2.16\times10^{-3} \pm 0.22\times10^{-3}$	↑ $+6.2\times10^{-4} \pm 2.3\times10^{-4}$
(μmol m^{-2} s^{-1})	(4.2u, IW)	8.9×10^{-4} (ns)	(10.0u, DD)	(2.7u, IW)

a.



b.



c.

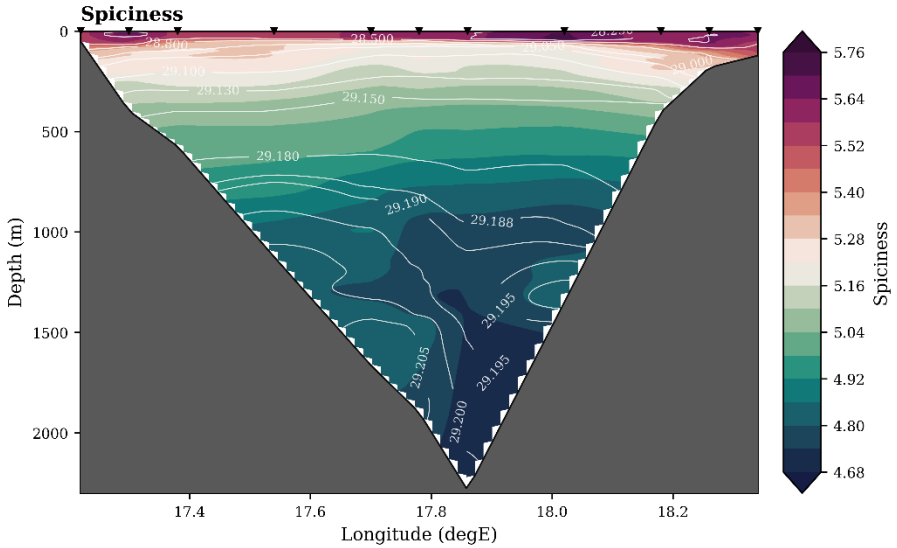


Figure S1: Atmospheric forcing and hydrographic context. (a) Mean wind-stress magnitude (N m⁻²) over the Gulf of Taranto for November 2023. (b) Monthly seasonal cycle of area-averaged wind-stress magnitude for 2023. (c) Vertical section of spiciness along the PIONEER-2023 transect, with potential-density-anomaly contours (σ_θ, kg m^{-3}).

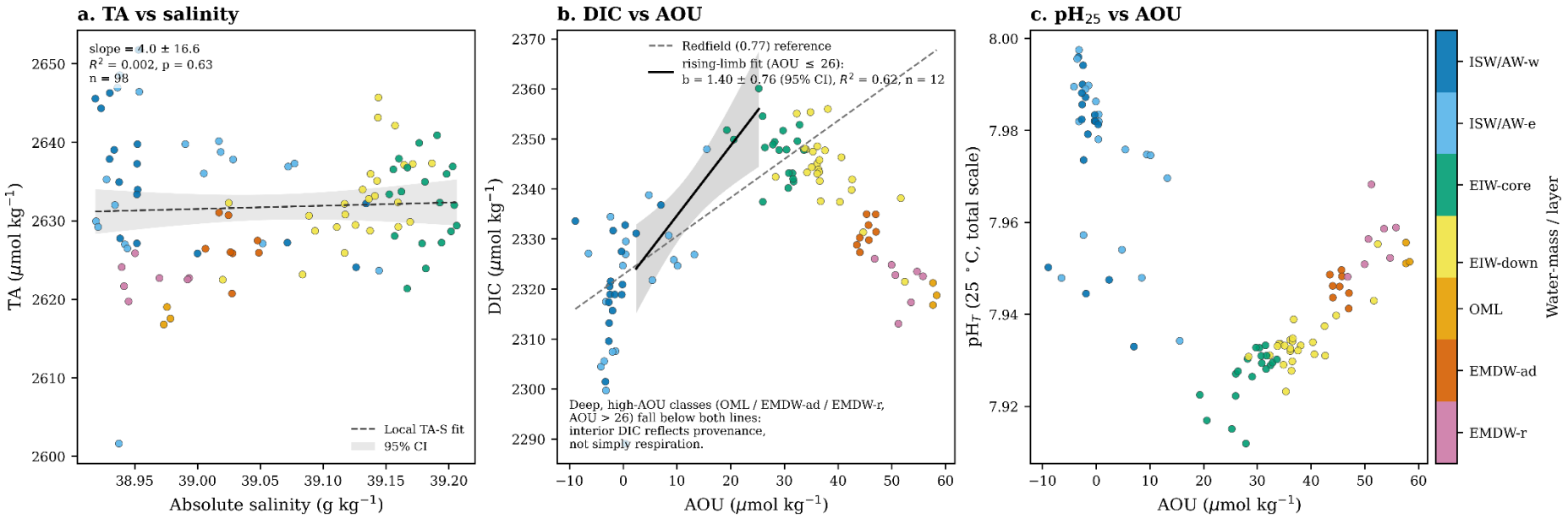


Figure S2: Carbonate-system property-property relationships for discrete bottle samples, coloured by hydrographic-biogeochemical class. (a) Total alkalinity (TA) versus Absolute Salinity (SA), with the section-wide linear fit (slope 4.0 ± 16.6 µmol kg⁻¹ per g kg⁻¹, R² = 0.002, p = 0.63, n = 98). The regression shows no detectable linear TA-SA relationship over the sampled range; it does not establish that TA is strictly invariant or identify the contributing endmembers. The absence of a slope reflects the organization of alkalinity by water mass rather than by salinity: the surface and deep classes occupy overlapping salinity ranges but differ systematically in alkalinity, while the intermediate classes carry the highest salinities at surface-like alkalinity. (b) Dissolved inorganic carbon (DIC) versus apparent oxygen utilization (AOU). The rising-limb fit for AOU = 2-26 µmol kg⁻¹ is b = 1.40 (95 % confidence interval 0.64–2.16), R² = 0.62, n = 12, and the sampled DIC maximum occurs at AOU = 25.7 µmol kg⁻¹. The interval encompasses both the Redfield et al. (1963) and the Anderson and Sarmiento (1994) reference stoichiometries and therefore does not discriminate between them. Beyond this maximum, DIC decreases and pH increases along the descending limb in the order EIW-down, EMDW-ad, EMDW-r, OML, with AOU increasing in the same order. The deep classes therefore depart from this upper-water fit, showing that one section-wide remineralization line is insufficient; provenance, mixing, and preformed properties remain possible explanations. (c) pH on the total scale at 25 °C (pH$_{25}$) versus AOU.

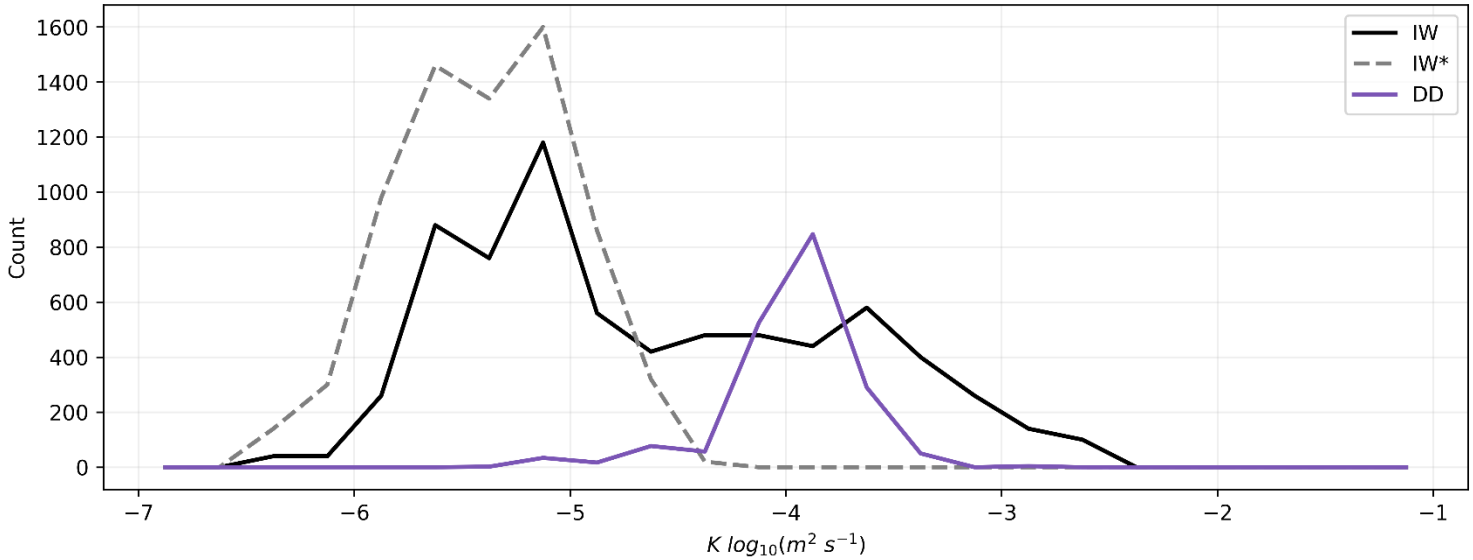


Figure S3: Frequency distributions of parameterized vertical diffusivity. Curves labelled IW and IW* represent the two internal-wave shear-strain diffusivity products, and DD represents the double-diffusive estimate.

References

Álvarez, M., Sanleón-Bartolomé, H., Tanhua, T., et al.: The CO_2 system in the Mediterranean Sea: a basin-wide perspective, Ocean Sci., 10, 69–92, https://doi.org/10.5194/os-10-69-2014, 2014.

Anderson, L. A. and Sarmiento, J. L.: Redfield ratios of remineralization determined by nutrient data analysis, Global Biogeochem. Cycles, 8, 65–80, https://doi.org/10.1029/93GB03318, 1994.

Cantoni, C., De Vittor, C., Faganeli, J., et al.: Carbonate system and acidification of the Adriatic Sea, Mar. Chem., 267, 104462, https://doi.org/10.1016/j.marchem.2024.104462, 2024.

Dentico, C., Cossarini, G., Civitarese, G., Giani, M., Rubino, A., and Cardin, V.: Air–sea CO_2 exchange in the Southern Adriatic Sea: assessing its role as a moderate carbon sink over the last decade (2015–2024), Biogeosciences, 23, 5399–5418, https://doi.org/10.5194/bg-23-5399-2026, 2026.

Redfield, A. C., Ketchum, B. H., and Richards, F. A.: The influence of organisms on the composition of sea-water, in: The sea, v. 2, edited by: Hill, M. N., Wiley, 26–77, 1963.
Terzić, E., Cardin, V., Le Meur, J., Dunić, N., Vodopivec, M., and Vilibić, I.: Unprecedented warming and salinization observed in the deep Adriatic, Limnol. Oceanogr. Lett., 10, 888–898, https://doi.org/10.1002/lol2.70051, 2025.